

SINGLE-COLUMN MODEL INTERCOMPARISON FOR A STABLY STRATIFIED ATMOSPHERIC BOUNDARY LAYER

J. CUXART¹, A. A. M. HOLTSLAG², R. J. BEARE³, E. BAZILE⁴,
A. BELJAARS⁵, A. CHENG⁶, L. CONANGLA⁷, M. EK⁸, F. FREEDMAN⁸,
R. HAMDI⁹, A. KERSTEIN¹⁰, H. KITAGAWA¹¹, G. LENDERINK¹²,
D. LEWELLEN¹³, J. MAILHOT¹⁴, T. MAURITSEN¹⁵, V. PEROV¹⁶,
G. SCHAYES⁹, G.-J. STEENEVELD², G. SVENSSON¹⁵, P. TAYLOR¹⁷,
W. WENG¹⁷, S. WUNSCH¹⁰ and K.-M. XU⁶

¹Univ. de les Illes Balears, Dpt. Física, Palma de Mallorca, Spain; ²Meteorology and Air Quality Section, Wageningen University, The Netherlands; ³Met Office, U.K.; ⁴Météo-France, Toulouse, France; ⁵European Centre for Medium-range Weather Forecast, Reading, U.K.; ⁶NASA Langley Research Center, Hampton, VA, U.S.A.; ⁷Univ. Politècnica de Catalunya, Dpt. Física Aplicada, Manresa, Spain; ⁸NOAA-NCEP, Camp Springs, MD, U.S.A.; ⁹Université Catholique de Louvain, IAG G. Lemaitre, Louvain la neuve, Belgium; ¹⁰Sandia National Laboratories, Livermore, CA, U.S.A.; ¹¹Japan Meteorological Agency, Tokyo, Japan; ¹²KNMI, Royal Netherlands Met. Institute, de Bilt, The Netherlands; ¹³West Virginia University, WV, U.S.A.; ¹⁴Meteorological Service of Canada, Dorval, Quebec, Canada; ¹⁵Stockholm University, Dpt. Meteorology, Stockholm, Sweden; ¹⁶Swedish Meteorological and Hydrological Institute, Norrköping, Sweden; ¹⁷York University, Canada

(Received in final form 21 February 2005)

Abstract. The parameterization of the stably stratified atmospheric boundary layer is a difficult issue, having a significant impact on medium-range weather forecasts and climate intergrations. To pursue this further, a moderately stratified Arctic case is simulated by nineteen single-column turbulence schemes. Statistics from a large-eddy simulation intercomparison made for the same case by eleven different models are used as a guiding reference. The single-column parameterizations include research and operational schemes from major forecast and climate research centres. Results from first-order schemes, a large number of turbulence kinetic energy closures, and other models were used. There is a large spread in the results; in general, the operational schemes mix over a deeper layer than the research schemes, and the turbulence kinetic energy and other higher-order closures give results closer to the statistics obtained from the large-eddy simulations. The sensitivities of the schemes to the parameters of their turbulence closures are partially explored.

Keywords: GABLS, Intercomparison, Mixing coefficients, Single-column models, Stably stratified flows, Turbulence parameterizations.

* E-mail: joan.cuxart@uib.es

1. Introduction

The planetary boundary layer (PBL) is the lowest part of the troposphere directly affected by the Earth's surface. When the surface is colder than the overlying air, the layer close to the ground becomes a stably stratified boundary layer (SBL). This usually happens at nighttime over land, when the surface cools due to longwave radiative emission, but also occurs during warm advection over colder surfaces.

Traditionally, the SBL is classified according to the intensity of the thermal stratification. The weakly stable SBL occurs when the winds are moderate to strong or the cloud coverage is high, resulting in weak vertical temperature gradients close to the ground, with sustained turbulence (Nieuwstadt, 1984). For more stable stratification, with weak winds and low cloud coverage, or in warm advection conditions, the turbulence weakens and the clear-air longwave radiation and local factors (such as the terrain heterogeneity and topography) become important. As the stratification increases, the mixing becomes sporadic or intermittent and often decoupled from the ground (Mahrt, 1999).

The representation of the SBL in atmospheric models is still rather poor (Viterbo et al., 1999; Holtslag, 2003). Changes in the turbulence schemes can lead to large differences of the near-surface temperature over land during winter, with significant impacts on medium-range weather forecasting or climate integrations. The drag at the surface depends on the SBL parameterization, and its misrepresentation can be felt at the largest scales, from entire continents, and also at synoptic scales where it provides the Ekman damping on cyclones (Beljaars and Viterbo, 1998). Many large-scale models use SBL schemes that provide stronger mixing than is implied by local observations or earlier research, including single-column simulation studies. This is felt to be due to the fact that, in very stable situations, the models do not mix enough at the lowest levels and enter a 'decoupled' mode, which can lead to run-away characteristics close to the ground (Viterbo et al., 1999). This issue has also been investigated by Derbyshire (1999) focussing on the influence on the strength of the geostrophic wind and the surface thermal conditions. Furthermore, too little mixing may produce too low drag at the surface, which could be detrimental to large-scale forecast performance.

The overall objective of the GEWEX Atmospheric Boundary Layer Study (GABLS – GEWEX stands for the Global Energy and Water Cycle Experiment) is to improve the understanding of the atmospheric boundary layer and its representation in regional and large-scale climate models. A simple shear-driven SBL case, already explored through a large-eddy simulation (LES) intercomparison (Beare et al., 2006), is chosen for a first evaluation of the performance of a number of operational schemes (that

is, schemes used within forecast or climate models) and of research or application oriented schemes. The LES intercomparison exercise provides controlled conditions to compare turbulence schemes using parameters that would rarely be at hand from the observations, such as the profiles of many turbulence quantities. A first example for the SBL is given by Galmarini et al. (1998), who use a one-dimensional (1D) model in comparison with LES. They find that their LES is in good approximate agreement with Nieuwstadt's theory on moderately stable turbulence regimes; however, the GABLS LES intercomparison shows that there remain difficulties in layers with relatively strong stratification, particularly near the ground and at the upper inversion.

Keeping these limitations in mind, we consider the LES intercomparison a suitable reference for this moderately stratified case. The differences between the LES models are relatively small and comparison to available observations (see Beare et al., 2006, Sections 3 and 5) indicates that they are all approximately in agreement with Nieuwstadt's theory although the mixing intensity is slightly overestimated. For stronger stratifications or more complex situations, state-of-the-art LES might not be as useful, and comparison with detailed observations, such as those provided by the CASES-99 experiment (Poulos et al., 2002) will be needed. Only one 'stability point' (in the bulk parameter space) is considered here because of the availability of LES data for this particular set-up and the large number of participating models. It is clear that a wider exploration from neutrality to strong stratification must be undertaken; the conclusions of this work, such as the sensitivity studies to the vertical resolution or to the closure constants, are necessarily of limited applicability.

In our study different operational and research schemes will be inter-compared, with the LES results used as a guiding reference. This follows earlier studies for unstable and neutral boundary layers (e.g Ayotte et al., 1996). Given the present level of understanding of turbulence, PBL models are still limited to crude approximations of reality. Further, even the best adjusted models in a research framework may not be appropriate when used as parametrizations within larger scale models. In principle, the operational models for medium- or long-range forecasts are adjusted to produce good overall forecasts, even at the cost of degrading skill in local areas. Schemes implemented in mesoscale models can focus more on good representation of small areas, since the possible detrimental effects at longer temporal scales are not relevant, but they still have to take into account the interaction with other active parameterizations. Finally, the models specifically built for PBL research are intended to reproduce at their best the different PBL regimes.

Here all the participating schemes are tested in the ideal PBL research framework. Relevant processes such as the dynamic or the surface forcings

are prescribed. Not all the important questions can be addressed here, for example the case prescribes the temporal evolution of the surface temperature, so that the decoupling issue cannot be explored. Differences in mixing efficiency can be discussed, however, exploring the behaviour of the momentum and heat fluxes, as well as some characteristics of the turbulence parameters provided by each scheme (mixing lengths, mixing coefficients and stability functions).

In Section 2, the case is described, and the description of the participating schemes is briefly given in Section 3. The results from each model are discussed and intercompared in Section 4, including the exploration of some details of the turbulence schemes. Finally, Section 5 describes the sensitivity to the closure parameters for some models and Section 6 gives a synthesis of the intercomparison exercise.

2. Description of the Case

This case is based on the simulations of an Arctic SBL by Kosovic and Curry (2000). The boundary layer is driven by an imposed barotropic geostrophic wind, with a specified surface cooling rate, and attains a quasi-steady state with a depth of between 150 and 250 m. It has also been used for a parallel LES intercomparison (Beare et al., 2005), aiming to quantify the reliability of stable boundary-layer LES. The same prescription has been retained for the single-column model intercomparison in order to minimise the sources of discrepancy between models and with the LES statistics. Nevertheless, weather-forecast or climate models have been included at their operational configuration.

A vertical domain of 400 m is used, with a grid mesh of 6.25 m (64 vertical levels), and a timestep of 10 s, to reduce the differences originating from the numerical discretization. A constant geostrophic wind with height, of 8 m s^{-1} in the x direction, is prescribed, and the latitude is 73° N ($f = 1.39 \times 10^{-4} \text{ s}^{-1}$). Radiation schemes are switched off and the duration of the run is nine hours. The initial state and the boundary conditions are

- The components of the wind are set equal to those of the geostrophic wind ($u = u_g$, $v = v_g$)-
- The potential temperature (θ) equals 265 K up to 100 m, then it increases at a rate of 0.01 K m^{-1} until the domain top, where a value of 268 K is reached. Moisture is not considered and therefore it is initialised to zero.
- For models requiring an initial turbulence kinetic energy (TKE or e) profile, it is set to $0.4(1 - z/250)^3 \text{ m}^2 \text{ s}^{-2}$ for $0 \leq z \leq 250 \text{ m}$ with an imposed minimum value above that.

- Surface boundary conditions: no slip (zero wind speed at z_0), with surface temperature (at z_0) specified as 265 K initially, decreasing at a constant rate of 0.25 K h^{-1} . The value of the aerodynamic roughness length (z_0) is set to 0.1 m for both momentum and temperature. The use of the following flux-gradient relations is recommended

$$\frac{\partial u}{\partial z} = \frac{\partial v}{\partial z} = \frac{u_*}{\kappa z} \left(1 + \beta_m \frac{z}{L}\right), \quad (1)$$

$$\frac{\partial \theta}{\partial z} = \frac{\theta_*}{\kappa z} \left(1 + \beta_h \frac{z}{L}\right), \quad (2)$$

with $\kappa=0.4$ the von Karman constant, $\beta_m=4.8$, $\beta_h=7.8$, where L is the Obukhov length, u_* is the friction velocity and θ_* is the surface temperature scale.

- Other constants: $g = 9.81 \text{ m s}^{-2}$, reference potential temperature $\theta_0 = 263.5 \text{ K}$, reference density $\rho_0 = 1.3223 \text{ kg m}^{-3}$ and surface pressure $p_{\text{ref}} = 1013.2 \text{ hPa}$.

3. Models Participating in the Intercomparison

Sixteen groups participated in the intercomparison and twenty different schemes have been used (see Tables I and II). The participant groups include seven National Weather Services, the European Centre for Medium-Range Weather Forecasts, seven Universities and two research centres and their collaborators. The names of the participant institutions and the acronyms used are given in Tables I and II. Four institutions submitted results from different schemes. Their acronyms are: ECMWF-MO, for the ECMWF results using prescribed flux-gradient relations close to the results of the Cabauw tower observations (Beljaars and Holtslag, 1991); LouvainU-L and LouvainU-eps for two 1.5-order schemes using a diagnosed mixing length and a dissipation equation respectively; the MetOffice-res, a research model different from the operational one; and the Stockholm University, whose similarity energy model is written StockholmU-sim. The KNMI model adds the acronym RACMO (Regional Atmospheric Climate Model).

Some of the schemes are the operational versions running in weather-forecast and climate models but run offline, whereas others are used in applications, within non-operational mesoscale models or for research purposes (see Table II). Most models have run using the prescribed temporal and spatial discretization, except ECMWF (and ECMWF-MO), MetOffice and NOAA-NCEP, which have used their operational grid (with 7, 6 and 8 points respectively within the prescribed vertical domain), and SandiaLabs, which used a very fine mesh (358 points). Some operational models cannot easily change their vertical resolutions since they are adjusted to them, but

TABLE I
Acronyms of the participant groups and scientists.

Acronym	Institution	Scientists
ECMWF	European Centre for Medium-Range Weather Forecasts	A. Beljaars
NOAA-NCEP	National Oceanic and Atmospheric Administration- National Centers for Environmental Prediction	F. Freedman M. Ek E. Bazile
MeteoFrance	Météo-France	H. Kitagawa
JMA	Japan Meteorological Agency	R. J. Beare
MetOffice	Met Office, UK	G-J. Steeneveld, A. A. M. Holtslag
WageningenU	Wageningen University	S. Wunsch, A. Kerstein
SandiaLabs	Sandia National Laboratories	J. Mailhot
MSC	Meteorological Service of Canada	G. Lenderink
KNMI	Royal Netherlands Meteorological Institute	J. Cuxart
UIB-UPC	University of the Balearic Islands- Politechnical University of Catalonia	L. Conangla
NASA	National Aeronautics and Space Administration	K-M. Xu, A. Cheng
WVU	West Virginia University	D. Lewellen
YorkU	York University	W. Weng, P. Taylor
LouvainU	Catholic University of Louvain	G. Schayes, R. Hamdi
SwedishMS	Swedish Meteorological and Hydrological Institute	V. Perov
StockholmU	Stockholm University	G. Svensson, T. Mauritsen

TABLE II
Model name, use, type and reference.

Model	Use	Type	Ref
ECMWF	Operational	1st order	Beljaars and Viterbo (1998)
ECMWF-MO	Operational-test	1st order	
NOAA-NCEP	Operational	1st order	Hong and Pan (1996)
MeteoFrance	Operational	1st order	Louis et al. (1982)
JMA	Operational	1st order	Mellor and Yamada (1974)
MetOffice	Operational	1st order	Louis (1979)
MetOffice-res	Research	1st order	Williams (2002)
WageningenU	Research	1st order	Duykerke (1991)
SandiaLabs	Research	ODT	Kerstein et al. (2001)
MSC	Operational	$e-l$	Belair et al. (1999)
KNMI-RACMO	Operational	$e-l$	Lenderink and Holtslag (2004)
UIB-UPC	Research	$e-l$	Cuxart et al. (2000)
	Mesoscale model		
NASA	Research	$e-l$	Xue et al. (2000)
	Mesoscale model		
WVU	Research	$e-l$	Sykes and Henn (1989)
YorkU	Research	$e-l$	Weng and Taylor (2003)
LouvainU-L	Research	$e-l$	Therry and Lacarrère (1983)
LouvainU-eps	Research	$e-\epsilon$	Duykerke (1988)
SwedishMS	Research	$e-\epsilon$	
StockholmU	Research	$e-l$	Andrén (1990)
StockholmU-sim	Research	$e-\theta^2$	Mauritsen et al. (2004)

the inspection of their behaviour in operational conditions is considered of interest as well. Many of the operational models used their own similarity functions in the surface layer instead of the recommended ones (indicated with an asterisk in Tables IV and V).

All the participating models, except the ODT scheme (standing for ‘one-dimensional turbulence’) of SandiaLabs, make use of the Reynolds decomposition in the equations of momentum and heat, and the turbulence is represented by fluxes, the vertical derivatives of the turbulence fluxes. These are parameterised assuming an equation formally like the diffusion equation, with eddy diffusivities K_m , K_h for momentum and heat

$$\overline{u'w'} = -K_m \frac{\partial u}{\partial z}, \quad (3)$$

$$\overline{v'w'} = -K_m \frac{\partial v}{\partial z}, \quad (4)$$

$$\overline{w'\theta'} = -K_h \frac{\partial \theta}{\partial z}, \quad (5)$$

where u , v are the mean horizontal wind components, θ is the potential temperature, and variables with primes stand for fluctuations about their respective horizontal means. Here we concentrate only on the parameterizations for the stably stratified regime. The turbulence schemes are classified according to their order of closure. Some of their characteristics are summarized in Table III.

3.1. FIRST-ORDER SCHEMES

Five of the seven operational schemes use first-order closures, based on Louis (1979) and Louis et al. (1982), along with individual modifications. In this case the fluxes are computed using

$$K_m = l_m^2 \frac{\partial U}{\partial z} f_m, \quad (6)$$

$$K_h = l_m l_h \frac{\partial U}{\partial z} f_h, \quad (7)$$

where l_m , l_h stand for the momentum and heat mixing lengths, and f_m , f_h are stability functions, U being here the wind speed. The differences between the first-order schemes arise mainly from the different approaches taken for the lengths and the stability functions. One exception is the NOAA-NCEP model, which uses a prescribed quadratic function for K_m below the boundary-layer height h , subject to the lower limit $K_m = 1 \text{ m}^2 \text{ s}^{-1}$. The MetOffice-res model diagnoses its mixing coefficients from stationary, locally scaled, second-order budgets. The lengths usually are forced to tend to κz in the surface layer and to some upper value λ_0 aloft (a parameter usually called the asymptotic length), using a formula proposed by Blackadar (1962) that gives more weight to the smallest value at the level of interest:

$$\frac{1}{l_m} = \frac{1}{\kappa z} + \frac{1}{\lambda_0} \quad (8)$$

for l_m and a similar expression for l_h if the lengths are different. The value of λ_0 is an adjustable parameter that varies between 40 and 200 m between models. None of the participants currently distinguish between the asymptotic length values for heat and for momentum. The stability functions vary between the first-order models and are the main factor that can explain differences between them. Most of them depend only on the local

TABLE III
Some characteristics of the turbulence schemes.

Model	K_m ($m^2 s^{-1}$)	K_h ($m^2 s^{-1}$)	Lengths (m)	Stab. functions (adim)
ECMWF (and ECMWF-MO)	$l_m^2 \frac{\partial U}{\partial z} f_m$	$K_m \frac{l_m f_h}{f_m}$	$l_{m,h}^{-1} = (kz)^{-1} + \lambda_0^{-1}$, $\lambda_0 = 150$ m	$f_m^{-1} = 1 + 10Ri(1 + 5Ri)^{-0.5}$ $f_h^{-1} = 1 + 15Ri(1 + 5Ri)^{0.5}$
NOAA-NCEP	$\frac{u_* k z}{f_m} (1 - z/h)^2$ as ECMWF	$K_m/1.32$ $K_m \frac{l_m f_h}{f_m}$	l_m, l_h as ECMWF with mods.	$f_m = \min(1 + 0.5h/L, 5)$ $f_m^{-1} = 1 + 10Ri(1 + 5Ri)^{-0.5}$ $f_h^{-1} = 1 + 15Ri(1 + 5Ri)^{0.5}$
Meteo France				LE (Yamada, 1975)
JMA	as ECMWF	as ECMWF	$l_m = l_h, \lambda_0 = 50$ m	$f_m = f_h = (1 + 10Ri)^{-1}$
MetOffice	as ECMWF	as ECMWF	as ECMWF, $\lambda_0 = \max(40., 0.15h)$	implicit in K_m, K_h
MetOffice-res	$K_m(z, h, u_*, L)$ as ECMWF	$K_h(z, h, u_*, L)$ as ECMWF	$l_{m,h}^{-1} = \frac{A}{z} + B \frac{N}{\sigma_m} + C \frac{S}{\sigma_m}$ $l_{m,h} = kz$	$f_m(\frac{z}{\Lambda}), f_h(\frac{z}{\Lambda})$ (Duynderke, 1991)
WageningenU	ND	ND	ND	ND
SandiaLabs	ND	ND	ND	ND
MSC	$0.516\sqrt{el_m}$	$K_m/0.85$	$l_m = \min(kz, 200)f_m$	$f_m = (1 + 12Ri)^{-1}$
KNMI-RACMO	$\sqrt{el_m}$	$\sqrt{el_h}$	$l_m(Ri, e, N), l_h(e, N)$	
UIB-UPC	$0.067\sqrt{el_m}$	$0.167\sqrt{el_h} f_h$	Bougeault and Lacarrère (1989) $l_\epsilon = l_m = l_h$	$f_h = (1 + C l_m^2 N^2 / e)^{-1}$
NASA	$0.1\sqrt{el_m}$	$K_m \min(3, F(l_m))$	$l_m = 0.76\sqrt{e/N^2}$	
WVU	$C_1\sqrt{el_m} f_m$	$C_2\sqrt{el_h} f_h$	$l_m = l_h = \min(h/4, 0.65z, \sqrt{e/2N^2})$	$f_m(Ri), f_h(Ri)$
YorkU	$0.55\sqrt{el_m}$	$K_m/0.85$	$l_m, l_\epsilon = F(z, L, \lambda_0)$	
LouvainU-L	$0.5\sqrt{el_m}$	$1.3K_m$	$l_m = l_h, l_\epsilon$ (Therry and Lacarrère, 1983)	
LouvainU-eps	$C_1 e^2 / \epsilon$	$K_h = K_m$	ND	
SwedishMS	$C_1 (Re) e^2 / \epsilon$	$K_h = K_m$	ND	
StockholmU	LE	LE	$l_m = l_h = l_\epsilon$	f_m, f_h (Andrén, 1990)
StockholmU-sim	LE	LE	$l_\epsilon^{-1} = (kz)^{-1} + \frac{N}{3.04\sqrt{e}} + \frac{S}{1.52\sqrt{e}}$	

L is the Obukhov length, N is the Brunt-Väisälä frequency, S is the wind shear and Λ is the local Obukhov length; LE stands for 'long expressions' and ND for 'not defined'. Further specifications can be found in the references listed in Table II.

gradient Richardson number, but some use local flux-gradient relations, and some make the first match the second in the surface layer.

The ODT scheme (Kerstein et al., 2001), instead of using a diffusion equation for the turbulence transport, applies a random sequence of rearrangements (mappings) applied to randomly selected intervals of the vertical grid, which may be viewed as an analogy of turbulent eddies. A model for the distribution of eddies is needed.

3.2. HIGHER-ORDER SCHEMES

The higher-order schemes are those that use one or more prognostic equations to compute the turbulence quantities. The e - l models are those that use a prognostic equation only for the turbulence kinetic energy (e). Two operational schemes (MSC and KNMI-RACMO) use such a proposal, together with two mesoscale models (UIB-UPC is implemented in Mesos-NH (Lafore et al., 1998), and NASA in ARPS (Xue et al., 2000)). Some of these schemes are, in fact, equilibrium second-order schemes, except for e (such as Stockholm U. or UIB-UPC), whereas the others prescribe the e equation and the lengths. We refer the reader to the original references and, to simplify the analyses, all the models with a prognostic TKE will be treated together. In this case, we could summarise the mixing coefficients as

$$K_m = c_m \sqrt{e} l_m f_m, \quad (9)$$

$$K_h = c_h \sqrt{e} l_h f_h, \quad (10)$$

$$\frac{\partial e}{\partial t} = -\overline{u'w'} \frac{\partial u}{\partial z} - \overline{v'w'} \frac{\partial v}{\partial z} + \frac{g}{\theta_{\text{ref}}} \overline{w'\theta'} - \frac{\partial \overline{w'e}}{\partial z} - c_\epsilon \frac{e^{3/2}}{l_\epsilon}, \quad (11)$$

where $c_m, c_h, c_\epsilon, c_e$ are constants and θ_{ref} is a reference value for the potential temperature. Equation (11) is the 1D turbulence kinetic energy equation, which uses a diffusion approach for the transport of e (usually with the same mixing coefficient as for the momentum fluxes, except for a constant c_e) and the Kolmogorov formula (Kolmogorov, 1941) for the dissipation (ϵ), which implicitly assumes isotropy and homogeneity. Since this last hypothesis is usually not applicable to the SBL, many models vary the value of the constant c_ϵ from 0.7 to a smaller value or use empirical parameterizations for the dissipation length l_ϵ .

The e - l models differ in three aspects: the values selected for the constants $c_m, c_h, c_\epsilon, c_e$, the parameterizations taken for the lengths and the stability functions. The Deardorff (1980) length for stable layers (proportional to \sqrt{e}/N) is used by many models (at least as a particular case). When a stability function is used, it might come from the complete system of second-order moment equations, but many times it is empirical or adjusted for the needs of each scheme. Some schemes assume a constant turbulence Prandtl number ($\text{Pr} = K_m/K_h$). The constants may vary between models by an

order of magnitude. It is clear that the number of possible combinations of these parameters, constants, lengths and stability functions, is very high, and one cannot isolate a single aspect. For the intercomparison of results in the next section, several diagnostics, such as equivalent stability functions or turbulence lengths, will be derived and discussed.

The e - ϵ models use, besides an e equation, an equation for the dissipation of e . The latter is a highly parameterised equation, that makes many assumptions (see Tennekes and Lumley, 1972) and that is widely used in engineering applications for neutrally stratified flows. The extension to stratified flows is difficult and two models are used here. LouvainUeps uses Duynkerke's formulation (1988), which states a special limitation on the dissipation production term related to buoyancy. On the other hand, the SwedishMS model makes the coefficients of the equation variable with the Reynolds number. For these schemes, in the e equation, the Kolmogorov formula is not used and ϵ is computed by

$$\frac{\partial \epsilon}{\partial t} = c_{\epsilon 1} \frac{\epsilon}{e} P(e) - \frac{\partial \overline{w' \epsilon}}{\partial z} - c_{\epsilon 2} \frac{\epsilon^2}{e}, \quad (12)$$

where $P(e)$ is the production term of the e equation, and $c_{\epsilon 1}, c_{\epsilon 2}$ are adjustable coefficients. The mixing coefficients are written

$$K_m = c_m \left(\frac{e^2}{\epsilon} \right) f_m, \quad (13)$$

$$K_h = c_h \left(\frac{e^2}{\epsilon} \right) f_h. \quad (14)$$

Finally, the Stock.U-sim model uses evolution equations both for e and $\overline{\theta'^2}$ together with a common dissipation length scale. The turbulent fluxes are computed from e and $\overline{\theta'^2}$ using energy similarity relations (Mauritsen et al., 2004)

$$\frac{\tau}{e} = f_1(\text{Ri}), \quad (15)$$

$$\frac{\overline{w' \theta'^2}}{\overline{\theta'^2} e} = f_2(\text{Ri}), \quad (16)$$

where Ri is the local gradient Richardson number, τ the total stress and f_1, f_2 are non-dimensional functions of the local flow stability only.

4. Results

As stated in the introduction, the different configurations of the participating models make a simple intercomparison difficult. Moreover, some operational models have simulated the case with their own specific flux-gradient

relations in the surface layer. Due to the prescription of the surface cooling rate, the decoupling issue cannot be explored; the latter is studied by Steeneveld et al. (2006). We will focus on the different magnitudes of the mixing coefficients of the schemes, particularly in relation to the vertical development of the SBL. Furthermore, the characteristics of the schemes will be intercompared and discussed.

The degree to which LES represents real SBLs has yet to be fully established, although LES results have been checked against available data from the Cabauw site in the Netherlands, through a convenient normalization. The LES results tend to produce slightly too much mixing, although the differences decrease when the resolution increases (Beare et al., 2005). Therefore, we have chosen to compare the single-column outputs to the statistics from the LES runs at a resolution of 3.125 m, since eight models have contributed at this resolution instead of the four models that submitted results at a resolution of 2 m; this gives a compromise between resolution and statistical representativity. The LES statistics provide reference values against which to compare.

4.1. DESCRIPTION OF THE MEAN AND TURBULENCE STRUCTURE OF THE SBL

A comparison of the results of the models is attempted here; Figure 1 provides the labels used in the figures for each model. In Figure 2, the time series of h and of the friction velocities indicate that the models reach a steady state after 5 h, similar to LES; h is defined as in the LES intercomparison: the height at which stress falls to 5% of its surface value, divided by 0.95. There is considerable spread among the LES results near the surface and at the boundary-layer top (at least compared to previous inter-comparisons for other regimes). This is most likely related to prescribing a surface temperature instead of a cooling rate. The spread among the single-column models is much larger. The SBL depth of the operational models is much higher than that from LES, whereas the research models produce a shallower SBL closer to the LES results. The friction velocities seem to be overestimated for the operational schemes, but the picture is not so clear as for h . The large boundary-layer heights and friction velocities for the operational schemes show that they have large exchange coefficients, thus transporting the characteristics of the air in the surface layer to the free atmosphere. These schemes miss some specific features such as the upper inversion that the LESs generate and that most of the research models also reproduce, as can be seen from the potential temperature profiles in Figure 3. In fact, elevated inversions within the SBL, similar to the ones here, have been found by Kosovic and Curry (2000) on the Arctic sea, by Garratt and Ryan (1989) in a warm advection over the sea south of Australia and by Lapworth (2003) over a U.K. site in the middle of the night.

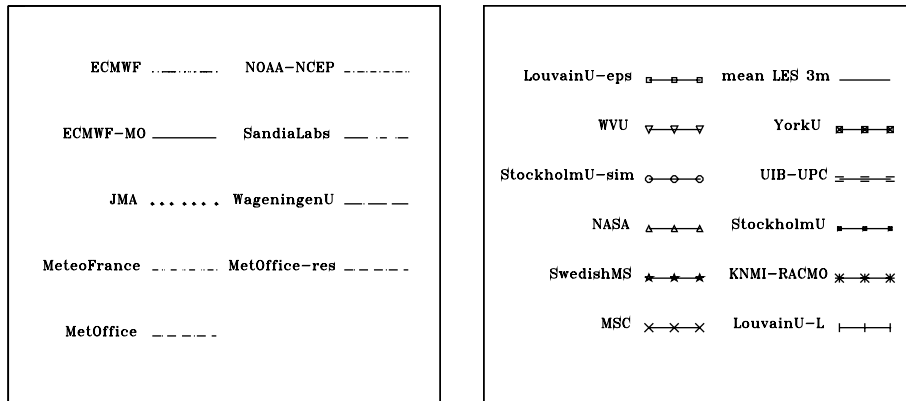


Figure 1. Labels for the first-order schemes (left) and for the higher order schemes (right). The LES will be represented by a shaded area when the LES averages plus/minus the standard deviation are plotted or with a thick continuous line when only the average is used.

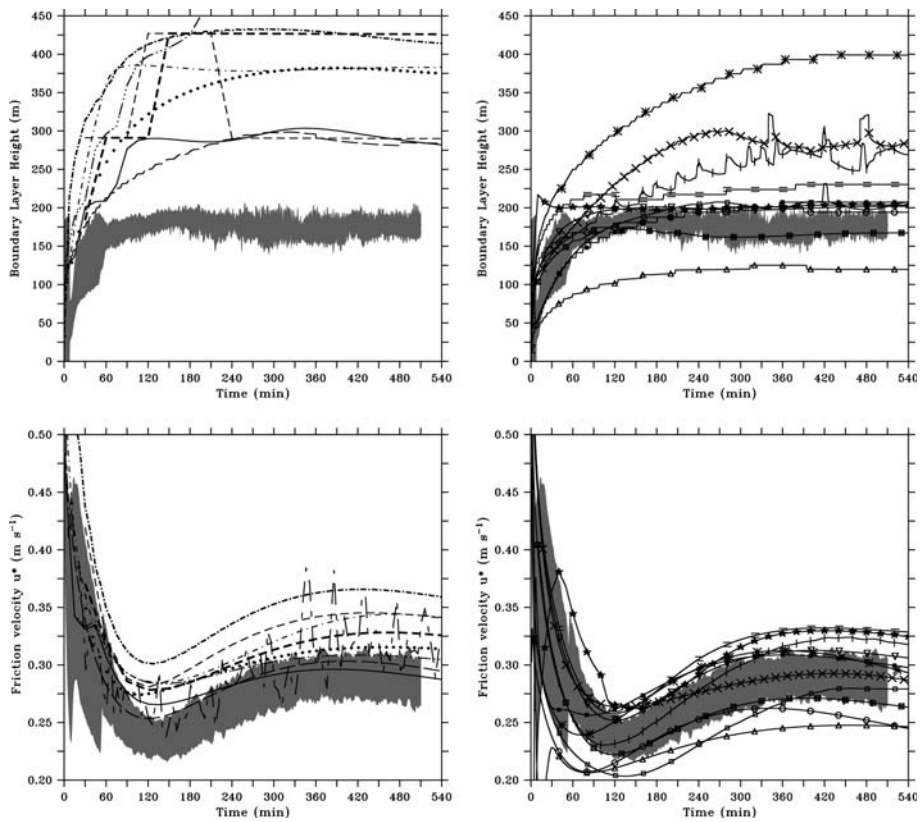


Figure 2. Time series for the boundary-layer height (top) and for the velocity friction (bottom). Left column: first-order schemes + ODT; right column: higher-order schemes.

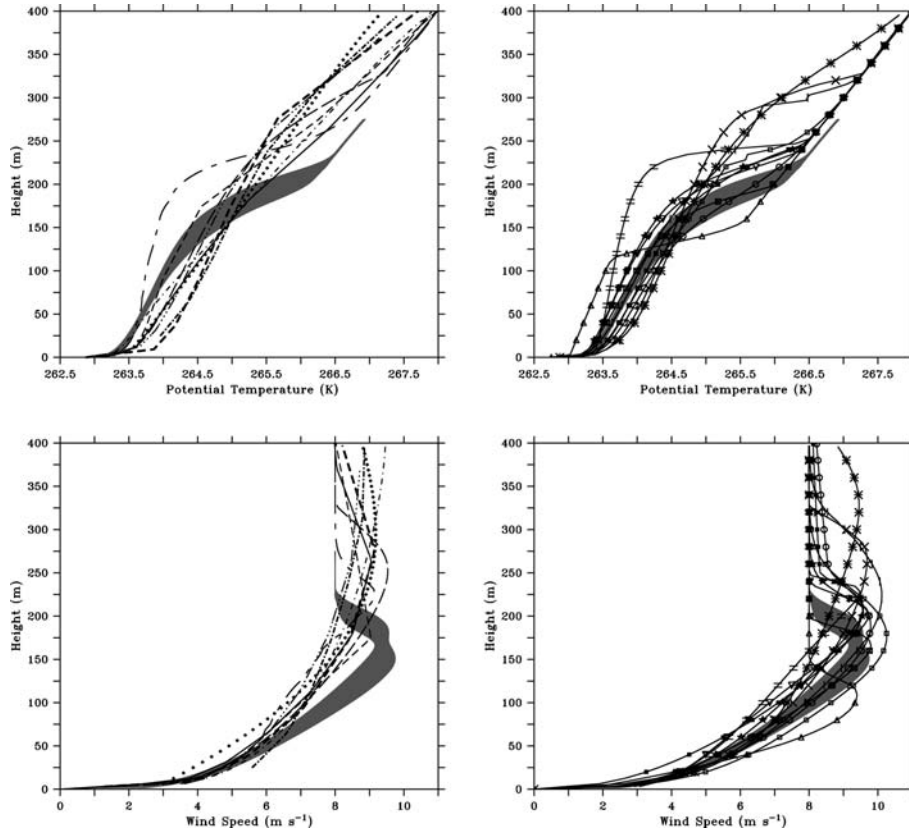


Figure 3. Potential temperature (top) and wind speed (bottom) averaged profiles for the ninth hour. Left column: first-order schemes + ODT; right column: higher-order schemes.

In Table IV the values at the end of the simulations for some parameters are given for each scheme. At the bottom of the table, the average and standard deviation values are found for the LES simulations and other model or categories. For h and the surface heat flux, all the categories have values larger than the LES, although the research and higher order categories are very close but with larger deviations. The Obukhov length indicates that all categories have slightly weaker stability in the surface layer than the LES. The friction velocity and the surface wind angle are well captured by the research and higher-order models, whereas the operational and first-order models give too high a friction velocity and smaller angles at the surface.

Some additional sensitivity tests were performed. The ECMWF model was run with surface similarity functions very close to the recommended ones, and it is shown in the Figures with the label ECMWF-MO. The

TABLE IV
Final values of some characteristics of the simulated SBL.

Model	h (m)	$\overline{w'\theta'_s}$ (K m s ⁻¹)	u_* (m s ⁻¹)	L (m)	Surface angle (°)
ECMWF +*	483	-0.018	0.31	106	21
ECMWF-MO	282	-0.011	0.29	150	27
NOAA-NCEP +*	416	-0.027	0.36	119	27
MeteoFrance +*	383	-0.013	0.34	204	23
JMA +	377	-0.021	0.31	102	34
MetOffice + *	426	-0.020	0.33	117	36
MetOffice-res *	290	-0.017	0.34	154	40
WageningenU	284	-0.013	0.30	136	30
SandiaLabs	ND	-0.018	0.32	132	33
MSC +	285	-0.016	0.29	102	29
KNMI-RACMO +*	399	-0.017	0.30	106	24
UIB-UPC ++	230	-0.017	0.33	138	35
NASA ++	120	-0.005	0.25	116	42
WVU	202	-0.013	0.31	155	37
YorkU	167	-0.010	0.27	123	36
LouvainU-L	270	-0.017	0.32	122	42
LouvainU-eps	208	-0.012	0.28	117	46
SwedishMS	204	-0.014	0.33	124	33
StockholmU	207	-0.011	0.30	156	38
StockholmU-sim	194	-0.009	0.25	109	32
LES 3.125 m (average; σ)	177; 16	-0.012; 0.002	0.29; 0.02	149; 31	35; 3
all 1D models (average; σ)	285; 108	-0.015; 0.005	0.30; 0.03	127; 25	33; 7
operational (average; σ)	396; 60	-0.019; 0.004	0.32; 0.03	122; 37	28; 6
research (average; σ)	208; 47	-0.013; 0.004	0.29; 0.03	130; 15	36; 5
first-order (average; σ)	395; 66	-0.019; 0.005	0.32; 0.02	131; 35	30; 6
higher order (average; σ)	226; 73	-0.013; 0.004	0.29; 0.03	125; 18	36; 6

(+): operational, (++): mesoscale, (*): not using prescribed similarity functions. At the end of the table, average and standard deviation values for categories of models.

amount of mixing and the vertical development of the mixing layer is reduced, in agreement with the research schemes. However, in an operational context, the reduced friction velocity often has a detrimental effect on forecast skill scores (Beljaars, 1995). Conversely, the JMA model, using the same prescribed functions, has a very deep SBL. The differences are probably due to the mixing length and stability functions.

Many of the aforementioned characteristics are confirmed by the profiles of the potential temperature, the wind speed and their turbulent fluxes (Figures 3 and 4). Most operational schemes overestimate mixing, are warmer than LES in the lower part of the SBL and colder above. The research first-order models, more or less, reproduce the upper inversion and ODT has too strong mixing below the inversion. The higher-order models cluster more closely although some of them have singular behaviour, such as UIB-UPC overestimating mixing below the upper inversion, or NASA having a too low SBL height. The MSC and KNMI-RACMO models along with the LouvainU-L have enhanced mixing up to higher levels.

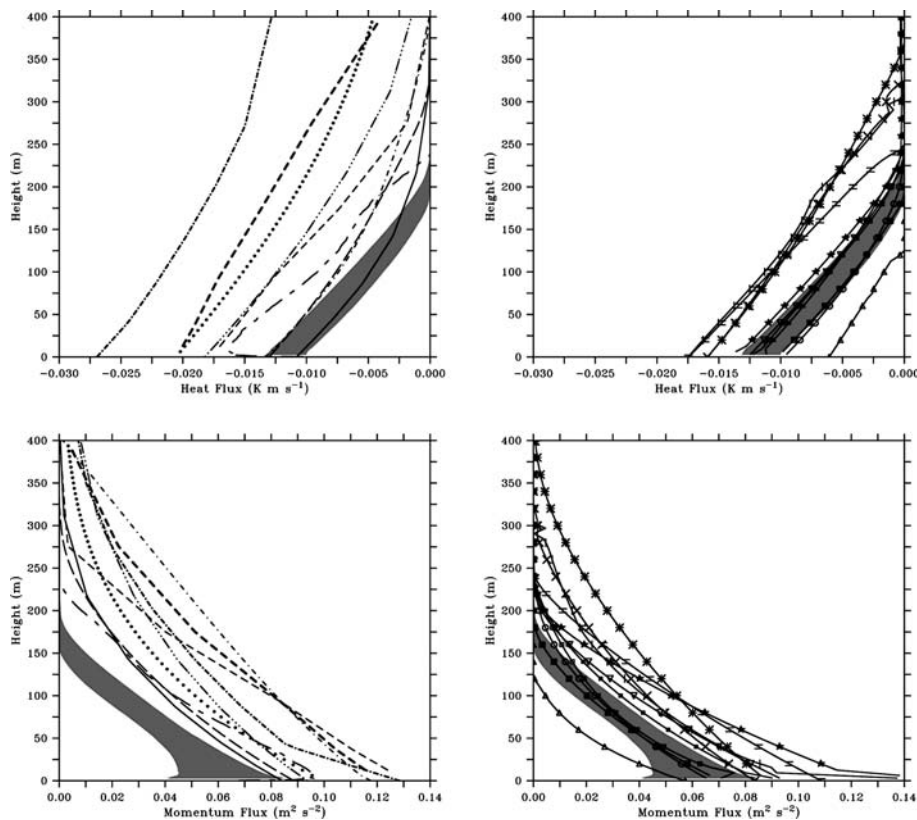


Figure 4. Heat flux (top) and momentum flux (bottom) as for Figure 3.

The Louvain models show step-like jumps at the inversion layer. In general, higher order models imply a critical Richardson number (Ri_c), explaining why the SBL does not grow as much as for the first-order models, which typically use larger cut-off (or no) values for Ri_c .

Similar comments can be made for the wind speed and momentum flux. The operational models, with too much mixing, are not able to generate a wind maximum near the SBL top as seen in LES, except for MSC. The differences in wind direction at the surface (last column in Table IV) are up to 25° ; such differences are significant for the forecasting of near-surface winds. There also seems to be a relation between h and the value of the cross-isobaric angle of the wind at the surface, which are further analysed in Svensson and Holtslag (2006). It can be seen in Figure 5 that the profiles of the turbulent fluxes when normalised by their surface value and h are very similar, decreasing linearly with height. They behave like LES, the Nieuwstadt theory and the observations, as shown in Figure 11 of Beare et al. (2006).

Table V shows that the LES results seem to imply two distinct interpretations of the boundary-layer depth: the height where the wind is maximum, very similar to h , and the level where the SBL fades away, since all the turbulence decays and the free atmosphere values are recovered (we could call it h_{top}); the first is located just below 200 m, whereas the second is above that height. The turbulence schemes do not behave with such a regularity and provide very different heights depending on the inspected parameter. Besides, the operational schemes tend to mix throughout the domain, so some of these measures cannot be defined. Nevertheless, about seven schemes behave in the upper inversion layer like LES. It is also interesting to note that the layer between the wind maximum and its geostrophic value varies a lot between models; the LESs indicate a layer

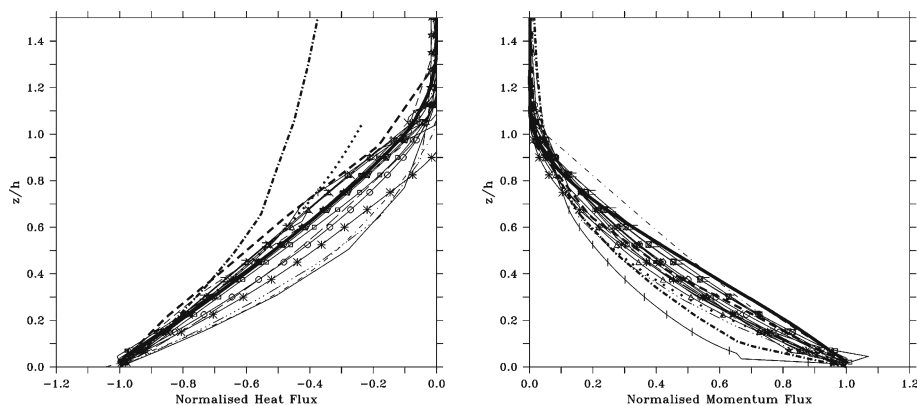


Figure 5. Heat flux (left) and momentum flux (right) as for Figure 3, normalised by the surface values (the height is normalised by the boundary-layer height).

TABLE V

Relevant heights (m): (1): boundary-layer height; (2): where the wind reaches the geostrophic value, (3): wind maximum, (4): where the momentum flux equals 1% of the surface value, (5): where the vertical gradient of temperature is that of the free atmosphere, (6): where the heat flux equals 1% of the surface value, (7): where the TKE reaches its minimum value.

Model	h (1)	Wind-geo (2)	Wind max (3)	MF (4)	Grad(T) (5)	HF (6)	TKE min (7)
LES 3.125 m	150–200	200–260	150–205	180–240	210–250	210–240	210–250
ECMWF +*	483	400+	370	400+	400+	400+	ND
ECMWF-MO	282	390	260	400	260	325	ND
NOAA-NCEP +*	416	400+	395	400+	400+	400+	ND
MeteoFrance +*	383	400+	400+	400	400+	386	ND
JMA +	377	400+	297	400+	400+	400+	ND
MetOffice +*	426	400+	276	400+	400+	400+	ND
MetOffice-res *	290	400	175	400	275	400	ND
WageningenU	284	331	250	290	330	325	ND
SandiaLabs	ND	281	226	236	285	239	ND
MSC +	285	328	266	319	325	325	255
KNMI-RACMO +*	399	400+	327	399	400+	368	370
UIB-UPC ++	230	253	228	238	250	250	240
NASA ++	120	153	109	119	160	125	120
WVU	202	241	203	222	240	228	225
YorkU	167	203	166	181	200	188	180
LouvainU-L	270	372	222	291	320	309	305
LouvainU-eps	202	309	178	222	290	234	230
SwedishMS	204	272	209	225	250	400+	220
StockholmU.	207	400+	206	234	250	247	230
StockholmU-sim	194	400+	188	228	200	234	195

(ND stands for not defined, 400+ means somewhere above 400 m.)

of depth between 25 and 40 m, whereas for the single-column models it can vary from just 25 m (UIB-UPC) to more than 100 m for MetOffice-res or LouvainU-L, for instance. This layer would deserve special attention in further studies since it is where the adjustment between the PBL and the free atmosphere takes place. Whether or not an inversion develops can modify greatly the efficiency of mixing in this layer.

4.1.1. *Sensitivity to the Resolution*

Some operational and research models were tested using a variety of temporal and spatial resolutions, typically vertical resolutions of 25, 50 and 100 m. They report results fairly insensitive to these changes in discretization for resolutions up to grid sizes of 50 m, although the sensitivity was larger to the location of the first computation point above the ground. A similar exercise can be found for the ECMWF in Beljaars (1992). The sensitivities of the operational schemes seem related to bulk parameters such as Ri_c or asymptotic lengths, indicating that the turbulent mixing within this SBL is strong enough for this stability measure, making the vertical resolution of secondary importance. For stronger stabilities the changes with resolution might be more significant, as well as in cases when the boundary layer is coupled to the surface (Steenefeld et al., 2006). The ECMWF-MO test with different surface-layer formulation has a large impact on the results, which are at low resolution, whereas for JMA there is not such sensitivity at high resolution. If the vertical resolution is higher than the Obukhov length, as for JMA, the surface-layer parameterization does not seem to matter much, and the important issue might be the parameterization in the interior of the SBL.

4.2. CHARACTERISTICS OF THE TURBULENCE SCHEMES

4.2.1. *Magnitude of Turbulent Diffusion*

One of the main objectives of the present work is to analyse the different mixing characteristics between the operational and the research models in comparison with LES. In Figure 6 the profiles of the mixing coefficients and of the turbulence Prandtl number and momentum stability functions are shown. The momentum eddy coefficients are (much) greater than the mean LES value for most of the models, although some higher order models are closer to LES. This explains why the wind profiles are too well mixed in general, and those models with strong coefficients at the upper part of the SBL do not have a wind maxima at the inversion. Most models show a linear behaviour with height near the ground and a maximum value at about a quarter to a third of the SBL depth. This ‘cubic’ shape for the eddy-diffusivity coefficient for momentum has been utilised before in synoptic-scale weather forecast and climate models (e.g., Troen and Mahrt, 1986; Holtslag and Boville, 1993; Hong and Pan, 1996). Notice also that the LES value is plotted just up to 160 m, because between that height and 190 m its computation becomes essentially a division of two small numbers since no significant wind shear exists around the wind maximum. Furthermore, the LES values are given without shaded deviation areas because the computation of the errors for those derived quantities gives very large standard deviations.

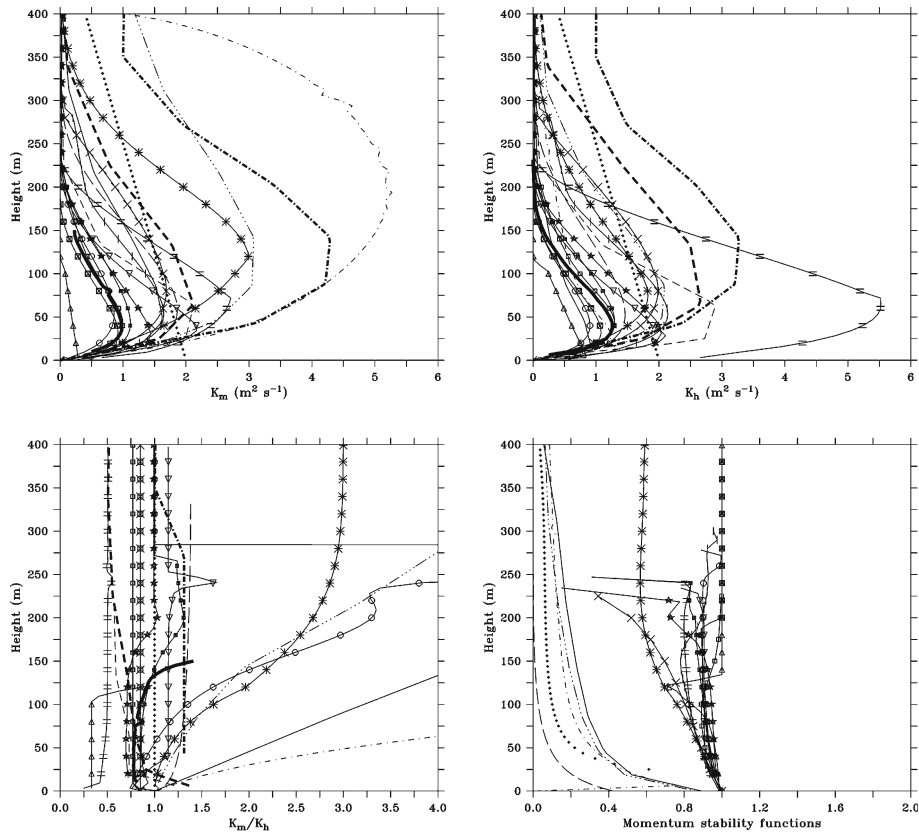


Figure 6. Momentum mixing coefficient (up left), heat mixing coefficient (up right), turbulence Prandtl number (bottom left) and stability function, and its equivalent for TKE models, (bottom right) for the ensemble of models.

The eddy-diffusivity coefficients for heat have shapes very similar to the momentum ones for most of the schemes, although maxima vary significantly. Models having large heat exchange coefficients at the top of the SBL do not generate the upper inversion. The turbulence Prandtl numbers show that the LESs provide an average value of about 0.8 until the base of the inversion; this LES-derived value is not plotted upwards because K_m is not available. The range of values for the Prandtl number of the schemes is very large, but most of the research models have almost constant values below the inversion, varying as much as from 0.3 to 1.6, whereas many operational ones have Prandtl numbers varying with height. It is clear that this is a major difference between the models. The models with Pr close to or below 0.5 suffer from too much mixing below the inversion, consistent with the findings of Derbyshire (1994).

For the TKE schemes, ‘first-order-like’ stability functions can be derived assuming steady-state condition for the TKE equation (Mellor and Yamada, 1982; Holtslag, 1998),

$$K_m = c\sqrt{e}l_m = c'l_m^2 \frac{\partial U}{\partial z} \sqrt{1 - \text{Ri}_f}, \quad (17)$$

where $\text{Ri}_f = \text{Ri}/\text{Pr}$ is the flux Richardson number. It can be seen that this expression is equivalent to the mixing coefficient for momentum for the first-order schemes (Equation (6)) where here $\sqrt{1 - \text{Ri}_f}$ would play the role of f_m (c and c' being arbitrary constants). The values of $\sqrt{1 - \text{Ri}_f}$ computed for all the higher-order schemes are shown in Figure 6 (bottom right), where the f_m values directly provided by some first-order models are also plotted (therefore not computed through $\sqrt{1 - \text{Ri}_f}$). The first-order models have values of f_m much smaller than the equivalent quantity for the higher-order models. In general, the former use lengths that do not take into account the stability, and tend to some relatively large asymptotic value above the surface layer, in contrast to the latter, and they may differ by an order of magnitude in the middle of the SBL. Therefore, the first-order schemes use their stability functions to adjust K_m to small values, whereas the higher-order ones use mostly the mixing length as their basic adjustable parameter.

4.2.2. Turbulence Lengths within the TKE-based Schemes

As stated in the description of the participating models, prognostic TKE schemes involve three distinct mixing lengths: one for momentum (l_m), one for heat (l_h) and one for dissipation (l_ϵ). As shown in Table III, these scales have a variety of formulations. Some models distinguish between all of them, some consider only one mixing length common for heat and momentum, and others use a unique master length, although with different constants or modifying functions. In order to be able to compare the different schemes, equivalent lengths are computed as

$$l_m = K_m / \sqrt{e}, \quad (18)$$

$$l_h = K_h / \sqrt{e}, \quad (19)$$

$$l_\epsilon = (c_\epsilon e^{1.5}) / \epsilon. \quad (20)$$

In this way, the joint contribution of the lengths and any other coefficient (such as a stability function or a closure constant) are given together and compared to the same quantity as provided by the LESs. The TKE for this case (not shown) is a quantity that decreases with height with values between 0.2 and $0.5 \text{ m}^2 \text{ s}^{-2}$ near the ground, the LES average value being around $0.3 \text{ m}^2 \text{ s}^{-2}$. The TKE budgets show that the steady state results of a quasi-equilibrium between the shear production and the

dissipation, the buoyancy destruction and the turbulence transport contributions are an order of magnitude smaller.

Figure 7 shows the three lengths. Again, the LES values are given without shaded deviation areas for the same reason given above. The momentum mixing length as provided by LESs is about 1 m and most models provide an equivalent length below 5 m within the SBL, with smaller values near the ground and at the inversion layer. The average heat mixing length provided by the LESs is slightly larger than the one for momentum below the inversion (2.5 m instead of 2 m at the maximum). The single column models do not distinguish much between the two lengths when the shape is observed, but they show a larger dispersion among them, similar to the Prandtl number. The UIB-UPC model has a factor of two between both lengths, very much consistent with its Prandtl number of about 0.5, and suggesting that a closure constant might be too large for heat in the non-strongly stratified SBL.

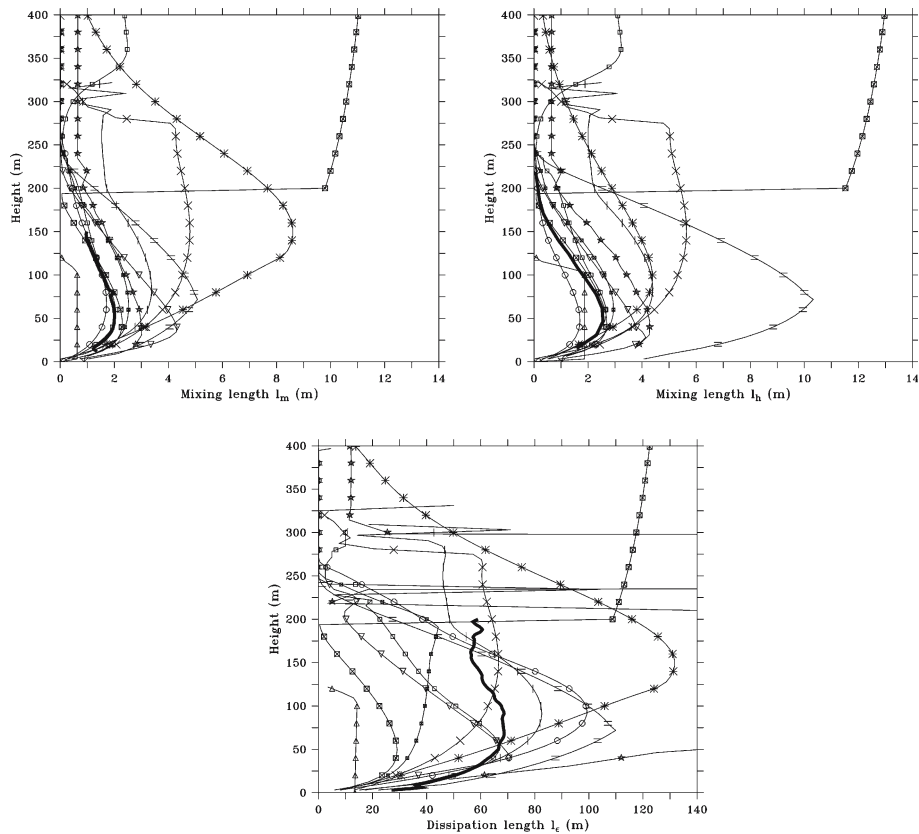


Figure 7. Equivalent mixing length for momentum (up left), for heat (up right) and equivalent dissipation length (bottom) for the higher order models.

For the equivalent dissipation length, the definition includes the value of c_ϵ . There is a large variety of proposed values for this coefficient; the value used in isotropic turbulence is 0.7, and Hunt et al. (1985) propose 0.4 for stably stratified conditions, where a strong case is made for its use. The participating schemes in this work take values varying from 0.08 to 0.7. This is why it is proposed to consider the coefficient c_ϵ inside the equivalent dissipation length. The LES values, regardless of the value considered for c_ϵ in the range discussed, are larger than the corresponding mixing lengths. If the dissipation length is taken as the scale of the more energetic eddies, it may range from about 10 to 50 m approximately in the SBL, with a horizontal contribution that can be significant at the inversion. However, this result derives from the ratio of two very small values at the top of the inversion and might be questionable. Nevertheless, Schumann (1991) states that it is reasonable to have small mixing lengths in stable conditions, but that the dissipation lengths might be larger due to the kinetic energy of wavy motion with little transfer to the smaller dissipative scales. On the other hand, the mixing length, much smaller, provides a scale of vertical mixing consistent with K theory based on the local characteristics of the layer. In general, the higher order turbulence schemes provide equivalent momentum and dissipation lengths of the same order of magnitude and similar shapes as the LESs.

5. Sensitivity to Closure Parameters

The differences between the results analysed above seem related to the values that each model uses for specific adjustable parameters rather than to different physically-sounded hypotheses in the schemes. To further explore this, additional runs were performed by nine models, aiming to find a better fit to the LES results. This exercise is specially relevant for those models that are implemented in global forecast, climate or mesoscale models, where there is no freedom to tune to a specific case. In fact, operational models might have values tuned to their specific requirements, maybe taking into account subgrid motions of mesoscale origin that cannot be accounted for by any other parameterization. Since only one stability point in the bulk parameter space is covered, the aim is not to improve the performance of the schemes in stably stratified conditions, but to show how sensitive they are to small (and quite arbitrary) changes in their free parameters. In Table VI, the models and the changes are summarised.

The changes involve mainly the following parameters: the limiting on the values of the lengths, the turbulent Prandtl number or the modification of some threshold values of the schemes, such as Ri_c . In Table VII, the relevant heights are given for the tuned runs. Both h and h_{top} are well defined here

TABLE VI
 Summary of modifications to models that were explored to bring the results into better agreement with those from LES.

Model	Change 1	Change 2	Change 3
NOAA-NCEP +*	reduce minimum K_m to 1.5×10^{-5}	reduce Ri_c to 0.25	refine mesh
MeteoFrance +*	1: cubic function in $[0-h]$	$f_h^{-1} = 1 + 15Ri\sqrt{1+25Ri}$	$f_m^{-1} = 1 + 10Ri/\sqrt{1+Ri}$
JMA +	reduce λ_0 to 10m	remove K_m, K_h bounding limits	
SandiaLabs	change eddy model	reduce mesh	
MSC +	change l to TL83	Take $Pr = 0.74$	
KNMI-RACMO +*	$Pr = 0.5$ (for stable limit)		
UIB-UPC ++	use λ_0 and l_{\min}		
NASA ++	$Pr = 0.74, 1.8c_m$		
StockholmU-sim	$l_c^{-1} = (\kappa z)^{-1} + \frac{N}{0.22\sqrt{\epsilon}}$	change l , use λ_0	

TABLE VII

Relevant heights (m, as in Table V) for the simulations performed with the modifications summarized in Table VI.

Model	h (1)	Wind-geo (2)	Wind max (3)	MF (4)	Grad(T) (5)	HF (6)	TKE min (7)
LES 3.125 m	150–200	200–260	150–205	180–240	210–250	210–240	210–250
NOAA-NCEP +*	225	335	235	230	240	235	ND
MeteoFrance +*	300	400+	275	400	400	390	ND
JMA +	175	210	175	190	210	200	ND
SandiaLabs	250	270	245	260	275	265	275
MSC +	185	250	185	200	225	210	200
KNMI-RACMO +*	185	400+	185	200	210	200	190
UIB-UPC ++	160	210	150	185	185	190	190
NASA ++	165	210	150	185	225	185	170
StockholmU-sim	170	225	175	185	185	190	190

for all models, and h_{top} is larger than h in every case. The tuned results, as expected, converge much more to the LES average outputs, as it can be seen in Figure 8. The higher order models achieve results very close to the LES averaged temperature and wind, whereas the operational first-order schemes manage to produce upper inversions in contrast to what happened before. In all cases, the changes are produced by relatively minor changes in the adjustable parameters of the schemes. SandiaLabs has tested a new model for the distribution of eddies allowing use of a much coarser distribution.

The operational models have mostly adjusted Ri_c and the turbulence Prandtl number. The mixing coefficient for the NOAA-NCEP scheme is greatly reduced and is able to generate an upper inversion setting a much smaller bounding value to K_m , and lowering Ri_c from 0.5 to 0.25. MeteoFrance’s major change is related to a new stability function, independent of Ri_c , that leads to much smaller Prandtl numbers. JMA modifies the asymptotic length and removes the bounding limits of the mixing coefficients. The two TKE operational models, KNMI-RACMO and MSC, achieve results much closer to the LES averages through the diminishing of the Prandtl numbers, and MSC takes another formulation for the lengths. So, the tuning for the operational models consisted of decreasing the Prandtl number towards the value provided by the LESs.

The two TKE schemes inside mesoscale models also produce a close match to the LES results with minor changes, introducing an asymptotic

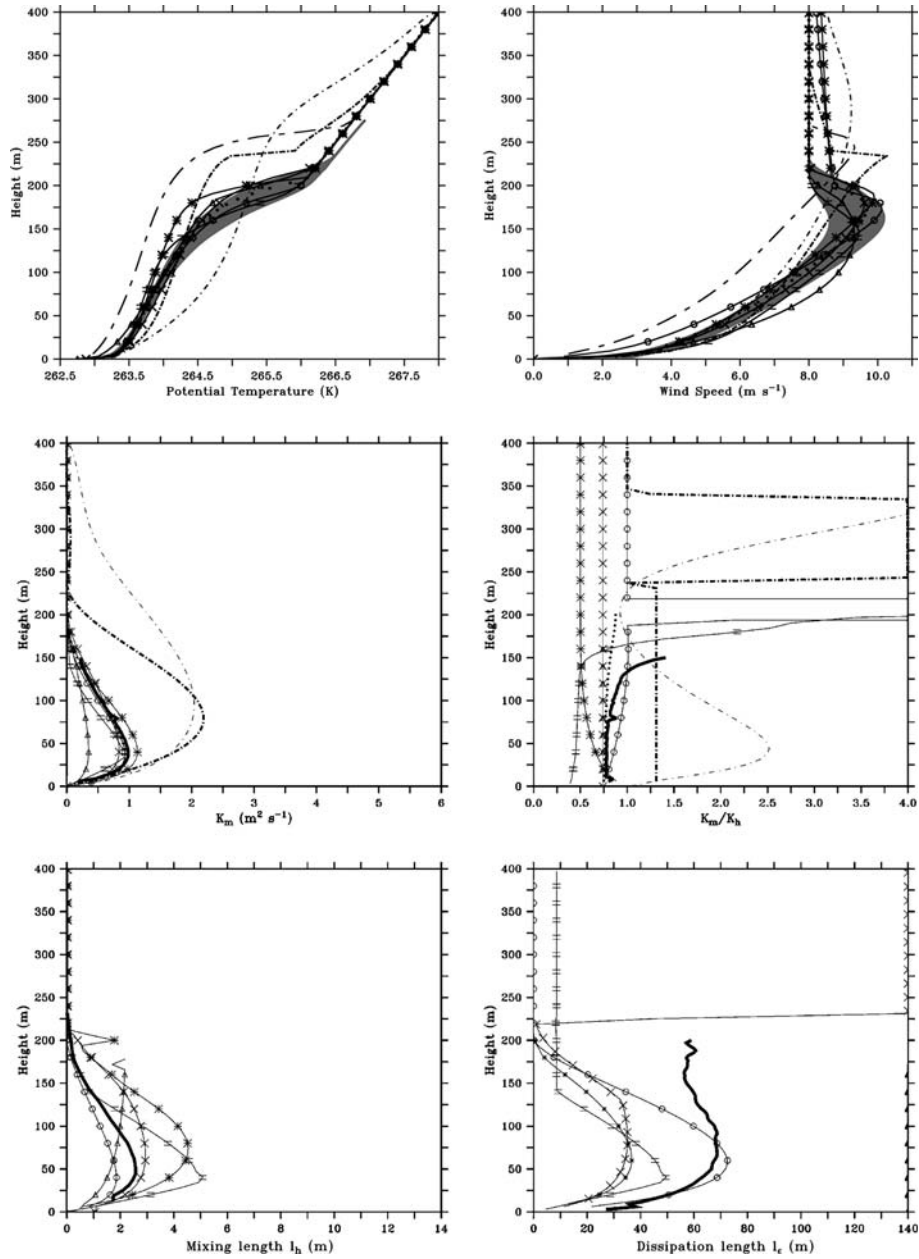


Figure 8. Potential temperature (top left), wind speed (top right), momentum mixing coefficient (middle left), turbulence Prandtl number (middle right), equivalent heat mixing length (bottom left) and equivalent dissipation length (bottom right) for the ensemble of the models participating in the tuning exercise.

length as the majority of the schemes, and NASA explicitly increases the Prandtl number to compensate for its too shallow SBL. The equivalent heat lengths for the higher order models do not vary much, only UIB-UPC has reduced significantly the length to about half its value. On the other hand, most models have diminished the values of the equivalent dissipation lengths, thus making their TKE equations more dissipative and the SBL less energetic, as the smaller values of the TKE (not shown) indicate.

6. Synthesis

This study has compared the different mixing efficiencies of several turbulence schemes for a moderately stratified SBL. In general, the operational models mix more than the research models with important consequences, such as the missing of the development of an upper inversion and the overestimation of the surface friction velocity. The first-order approaches use very similar formulations except for the values of some adjustable parameters, such as the mixing lengths or the stability functions. The operational TKE schemes also overestimate the mixing, but to a smaller extent. The research schemes, on the other hand, give results closer to the LES statistics. The behaviour of the models differs significantly above the upper inversion, as well as in the values for the surface-layer parameters.

Many research models use a prognostic TKE equation. Equivalent mixing lengths for heat, momentum and dissipation have been computed from LESs and for each model. The mixing lengths have values below 5 m, while the dissipation ones are larger. In the schemes, this difference is partially taken into account through the different values of the mixing and the dissipation closure constants. Two models use an additional prognostic equation for the dissipation, in both cases adapted for stably stratified flows, and one model uses an equation for the potential temperature variance. Furthermore, the model of SandiaLabs uses a totally different approach. The results of these models are also within the range of the other participants.

The participating schemes share many characteristics within each category and the differences lie mostly in the adjustable parameters. These basically affect the stability functions for the first-order schemes and the mixing lengths for the higher-order ones. The implementation of a scheme in operational, climate or mesoscale frameworks conditions includes choices of the tunable parameters, since they are usually adjusted to fit well with the other interacting parameterizations in models or to compensate for misrepresented processes. This fact makes it difficult to propose specific values for the tunable parameters from just this case.

It seems relevant that the differences lie basically in the values for tunable parameters. However the sensitivity exercise shows that the use of a

value for the turbulence Prandtl number close to that provided by the LESs makes the overall results of the schemes converge to the LES statistics. Furthermore, the exercise shows that the use of limiting values for the mixing lengths is convenient for the TKE schemes, whereas the equivalent dissipation length is larger than the mixing length when the schemes are adjusted for the case.

The vertical resolution does not appear to be an important issue for this SBL, since the results of the higher-order schemes do not change much even with a grid mesh of 50 m, and the first-order schemes did not report a significant sensitivity either. This is consistent with the fact that bulk parameters such as Ri_c or the closure constants do play a role in the sensitivity tests. This conclusion cannot be extrapolated to the strongly stratified case.

Even for this simple case some issues still remain unresolved, such as the behaviour at the upper part of the inversion. Also, the problems of SBL decoupling from the land surface and higher stability need to be examined. This motivates a future intercomparison more closely based on observations over land.

Acknowledgements

Toni Mira (UIB) is specially acknowledged for all his help in producing the final figures, also with the contribution of Maria Antònia Jiménez. The LES modellers are thanked for providing the outputs of their models, in particular Anne McCabe (Met Office) who provided the statistics from the LES intercomparison. The authors wish to acknowledge use of the Ferret program for the graphics in this paper and the help given by the user's support team at NOAA. David Lewellen has been supported in part by grant N00014-98-1-0595 from the U.S. Office of Naval Research. Laura Conangla and Joan Cuxart participation has been partially funded through project REN2002-00486 of the Spanish Government. Thorsten Mauritsen and Gunilla Svensson have been supported by the Swedish research council. The anonymous reviewers have greatly improved the contents of the paper, suggesting new ideas and alternative explanations for some of the results.

References

- Andrén, A.: 1990, 'Evaluation of a Turbulence Closure Scheme Suitable for Air-Pollution Applications', *J. Appl. Meteorol.*, **29**, 224–239.
- Ayotte, K. W., Sullivan, P. P., Andrén, A., Doney, S. C., Holtslag, A. A. M., Large, W. G., McWilliams, J. C., Moeng, C. H., Otte, M. J., Tribbia, J. J., and Wyngaard, J. C.: 1996, 'An Evaluation of Neutral and Convective Planetary Boundary-Layer Parameterizations Relative to Large Eddy Simulations', *Boundary-Layer Meteorol.*, **79**, 131–175.

- Beare, R. J., MacVean, M. K., Holtslag, A. A. M., Cuxart, J., Esau, I., Golaz, J.-C., Jimenez, M. A., Khairoutdinov, M., Kosovic, B., Lewellen, D., Lund, T. S., Lundquist, J. K., McCabe, A., Moene, A. F., Noh, Y., Raasch, S., and Sullivan, P. P.: 2006, 'An Intercomparison of Large-Eddy Simulations of the Stable Boundary Layer', *Boundary-Layer Meteorol.* In Press.
- Bélair, S., Mailhot, J., Strapp, J. W., and MacPherson, J. I.: 1999, 'An Examination of Local Versus Non-Local Aspects of a TKE-based Boundary Layer Scheme in Clear Convective Conditions', *J. Appl. Meteorol.*, **38**, 1499–1518.
- Beljaars, A. C. M. and Holtslag, A. A. M.: 1991, 'Flux Parameterization Over Land Surfaces for Atmospheric Models', *J. Appl. Meteorol.*, **30**, 327–341.
- Beljaars, A. C. M.: 1992, 'Numerical Schemes for Parameterizations', *ECMWF seminar Proceedings on Numerical Methods in Atmospheric Models*, Reading, U.K., 9–13 September 1991, Vol II, 1–42.
- Beljaars, A. C. M.: 1995, 'The Impact of Some Aspects of the Boundary Layer Scheme in the ECMWF Model', *ECMWF Seminar Proceedings on Parameterization of Subgrid Scale Physical Processes*, Reading, U.K., September 1994, 125–161.
- Beljaars, A. C. M. and Viterbo, P.: 1998, 'Role of the Boundary Layer in a Numerical Weather Prediction Model', (A.A.M. Holtslag and P.G. Duynkerke, eds), *Clear and Cloudy Boundary Layers*, Royal Netherlands Academy of Arts and Sciences, Amsterdam, 287–304.
- Blackadar, A. K.: 1962, 'The Vertical Distribution of Wind and Turbulent Exchange in a Neutral Atmosphere', *J. Geophys. Res.* **67**, 3095–3102.
- Bougeault, P., and Lacarrère, P.: 1989, 'Parameterization of Orography-Induced Turbulence in a Mesobeta-Scale Model', *Mon. Wea. Rev.* **117**(8), 1872–1890.
- Cuxart, J., Bougeault, P., and Redelsperger, J. L.: 2000, 'A Turbulence Scheme Allowing for Mesoscale and Large-Eddy Simulations', *Quart. J. Roy. Meteorol. Soc.* **126**, 1–30.
- Deardorff, J. W.: 1980, 'Stratocumulus-Capped Mixed Layers Derived from a Three-Dimensional Model', *Boundary-Layer Meteorol.* **18**, 495–527.
- Derbyshire, S. H.: 1994, 'A 'balanced' Approach to Stable Boundary Layer Dynamics', *J. Atmos. Sci.* **51**, 3486–3504.
- Derbyshire, S. H.: 1999, 'Boundary Layer Decoupling Over Cold Surfaces as a Physical Boundary Instability', *Boundary-Layer Meteorol.* **90**, 297–325.
- Duynkerke, P. G.: 1988, 'Application of the E-e Turbulence Closure Model to the Neutral and Stable Atmospheric Boundary Layer', *J. Atmos. Sci.* **45**, 865–880.
- Duynkerke, P. G.: 1991, 'Radiation fog: a comparison of model simulations with detailed observations', *Mon. Wea. Rev.* **119**, 324–341.
- Galmarini, S., Beets, C., Duynkerke, P. G., and Vila-Guerau de Arellano, J.: 1998, 'Stable Nocturnal Boundary Layers: a comparison of one-dimensional and large-eddy simulation models', *Boundary-Layer Meteorol.* **88**, 181–210.
- Garratt and Ryan: 1989, 'The Structure of the Stably Stratified Internal Boundary Layer in Offshore Flow Over the Sea', *Boundary-Layer Meteorol.* **47**, 17–40.
- Holtslag, A. A. M., and Boville, B.: 1993, 'Local Versus Nonlocal Boundary-Layer Diffusion in a Global Climate Model', *J. Climate* **6**, 1825–1842.
- Holtslag, A. A. M.: 1998, 'Modelling of Atmospheric Boundary Layers', (A. A. M. Holtslag and P. G. Duynkerke, eds), *Clear and Cloudy Boundary Layers*, Royal Netherlands Academy of Arts and Sciences, Amsterdam, 85–110.
- Holtslag, A. A. M.: 2003, 'GABLS Initiates Intercomparison for Stable Boundary Layers', *GEWEX news* **13**, 7–8.
- Hong, S. Y., and Pan, H. L.: 1996, 'Non-local Boundary Layer Vertical Diffusion in a Medium-Range Forecast Model', *Mon. Wea. Rev.* **124**(10), 2322–2339.

- Hunt, J. C. R., Kaimal, J. C., and Gaynor, J. E.: 1985, 'Some Observations of Turbulence Structure in Stable Layers', *Quart. J. Roy. Meteorol. Soc.*, **111**, 793–815.
- Kerstein, A. R., Ashurst, W. T., Wunsch, S., and Nilsen, V.: 2001, 'One-dimensional Turbulence: Vector Formulation and Application to free shear flows', *J. Fluid Mech.*, **447**, 85–109.
- Kolmogorov, A. N.: 1941, 'Dissipation of Energy in a Locally Isotropic Turbulence', *Doklady Akad. Nauk SSSR* **32**, 141.
- Kosovic, B., and Curry, J. A.: 2000, 'A Large Eddy Simulation Study of a Quasi-Steady, Stably Stratified Atmospheric Boundary Layer', *J. Atmos. Sci.* **57**, 1052–1068.
- Lafore, J. P., Stein, J., Asencio, N., Bougeault, P., Ducrocq, V., Duron, J., Fischer, C., Hérelil, P., Mascart, P., Masson, V., Pinty, J. P., Redelsperger, J. -L., Richard, E., and Vilà-Guerau de Arellano, J.: 1998, 'The Meso-NH Atmospheric Simulation System. Part I: Adiabatic Formulation and Control Simulations.', *Ann. Geophys.* **16**, 90–109.
- Lapworth, A. A.: 2003, 'Factors Determining the Decrease in Surface Wind Speed Following the Evening Transition', *Quart. J. Roy. Meteorol. Soc.*, **129**, 1945–1968.
- Lenderink, G., and Holtslag, A. A. M.: 2004, 'An Updated Length Scale Formulation for Turbulent Mixing in Clear and Cloudy Boundary Layers', *Quart. J. Roy. Meteorol. Soc.*, in press.
- Louis, J. F.: 1979, 'A Parametric Model of Vertical Fluxes in the Atmosphere', *Boundary-Layer Meteorol.* **17**, 187–202.
- Louis, J. F., Tiedtke, M., and Geleyn, J. F.: 1982, 'A Short Story of the Operational PBL Parameterizations at ECMWF', *Proc. Workshop on Boundary Layer Parameterization*, ECMWF, Reading, 59–79.
- Mahrt, L.: 1999, 'Stratified Atmospheric Boundary Layers', *Boundary-Layer Meteorol.* **90**, 375–396.
- Mauritsen, T., Svensson, G., Enger, L., Zilitinkevich, S., and Grisogono, B.: 2004, 'Energy Similarity - A New Turbulence Closure Model for Stable Boundary Layers', Preprints *16th AMS Conference on Boundary Layers and Turbulence*, Portland, Maine, 9–13 August 2004.
- Mellor, G. L., and Yamada, T.: 1974, 'A Hierarchy of Turbulence Closure Models for Planetary Boundary Layers', *J. Atmos. Sci.* **31**, 1791–1806.
- Mellor, G. L., and Yamada, T.: 1982, 'Development of a Turbulence Closure Model for Geophysical Fluid Problems', *Rev. Geophysics. Space. Phys.* **20**, 851–875.
- Nieuwstadt, F. T. M.: 1984, 'The Turbulent Structure of the Stable, Nocturnal Boundary Layer', *J. Atmos. Sci.* **41**, 2202–2216.
- Poulos, G. S., Blumen, W., Fritts, D. C., Lundquist, J. K., Sun, J., Burns, S. P., Nappo, C., Banta, R., Newsom, R., Cuxart, J., Terradellas, E., Balsley, B., and Jensen, M.: 2002, 'CASES-99: a comprehensive investigation of the Stable nocturnal boundary layer', *Bull. Amer. Meteorol. Soc.* **83**, 555–581.
- Schumann, U.: 1991, 'Subgrid Length-scales for Large-Eddy Simulation of Stratified Turbulence', *Theor. Comput. Fluid Dyn.* **2**, 279–290.
- Steenekeld, G. J., van der Wiel, B. J. H., and Holtslag, A. A. M.: 2006 'Modelling the Arctic Nocturnal Stable Boundary Layer and its Coupling to the Surface', *Boundary-Layer Meteorol.* in press.
- Svensson, G., and Holtslag, A. A. M.: 2006 'Impact of Turbulence in the Stable Boundary Layer on the Synoptic Scale Flow' *Boundary-Layer Meteorol.* in press.
- Sykes, R. I., and Henn, D. S.: 1989, 'Large-Eddy Simulation of Turbulent Sheared Convection', *J. Atmos. Sci.* **46**, 1106–1118.
- Tennekes, H., and Lumley, J. L.: 1972, *A First Course in Turbulence*, MIT Press, Cambridge, 300 pp.

- Therry, G., and Lacarrère P.: 1983, 'Improving the Eddy Kinetic Energy Model for Planetary Boundary Layer Description', *Boundary-Layer Meteorol.* **25**, 63–88.
- Troen, I., and Mahrt, L.: 1986, 'A Simple Model of the Atmospheric Boundary Layer: sensitivity to surface evaporation', *Boundary-Layer Meteorol.* **37**, 129–148.
- Viterbo, P., Beljaars, A. C. M., Mahfouf, J -F., and Teixeira, J.: 1999, 'The Representation of Soil Moisture Freezing and its Impact on the Stable Boundary Layer', *Quart. J. Roy. Meteorol. Soc.* **125**, 2401–2426.
- Weng W., and Taylor P. A.: 2003, 'On Modelling the One-Dimensional Atmospheric Boundary Layer', *Boundary-Layer Meteorol.*, **107**, 371–400;
- Williams, A. G.: 2002, 'Local Mixing with External Control in the Met Office Unified Model Stable Boundary Layer', Preprints *15th AMS Conference on Boundary Layers and Turbulence*, Wageningen, The Netherlands, 15–19 July 2002, pp. 311–312.
- Xue, M., Drogemeier, K. K., and Wong, V.: 2000, 'The Advanced Regional Prediction System (ARPS) – A Multi-Scale Non-Hydrostatic Atmospheric Simulation and Prediction Model. Part I: Model Dynamics and Verification', *Meteorol. Atmos. Phys.* **75**, 161–193.
- Yamada, T.: 1975, 'The Critical Richardson Number and the Ratio of the Eddy Transport Coefficients Obtained from a Turbulence Closure Model', *J. Atmos. Sci.*, **32**, 926–933.